

Synthesis and Evaluation of Magnesium and Zinc-Doped Hydroxyapatite-Banana Flower Extract-PLGA Composite for Bone Regeneration

MUNUSAMY SURESH^{1,2}, PALANISAMY KARTHIKEYAN³ and PULLAR VADIVEL^{4,*}

¹Department of Chemistry, Sri Sarada Niketan College of Arts and Science for Women, Salem-636354, India

²Department of Chemistry, Periyar University, Salem-636011, India

³Department of Chemistry, Government Arts and Science College, Idappadi, Salem-637102, India

⁴Department of Chemistry, Salem Sowdeswari College, Salem-636010, India

*Corresponding author: E-mail: vadivelsalem@gmail.com

Received: 13 December 2024;

Accepted: 20 January 2025;

Published online: 31 January 2025;

AJC-21899

Strategies for bone tissue regeneration need methods that provide an osteogenic environment conducive to bone formation. This study examines the synthesis and characterization of a new biocomposite material consisting of magnesium and zinc-doped hydroxyapatite (MZHAp), banana flower extract (BFE) and poly(lactic-co-glycolic acid) (PLGA) for possible applications in bone tissue engineering. The synthesized material was analyzed using FTIR, XRD, SEM-EDAX and microhardness assessments. The findings indicated effective incorporation of BFE and PLGA into the MZHAp matrix, resulting in increased crystallinity, superior mechanical characteristics and regulated shape. *In vitro* investigations, including cell survival, alkaline phosphatase (ALP) activity and alizarin red S (ARS) staining, demonstrated superior biocompatibility and considerable osteogenic potential of the MZHAp-BFE-PLGA composite. Moreover, the biocomposite demonstrated significant antibacterial efficacy against both Gram-positive and Gram-negative microorganisms. The results indicate that the MZHAp-BFE-PLGA composite may serve as a promising biomaterial for bone tissue regeneration applications.

Keywords: Antibacterials, Biocomposite, Biocompatibility, Zinc, Magnesium, Hydroxyapatite.

INTRODUCTION

Hydroxyapatite (HAp), a naturally occurring mineral known for its outstanding ability to interact well with living tissues, has been widely used in the field of biomaterials for a significant period of time [1]. Due to its similarity in structure to bone and teeth, as well as its ability to promote bone growth, it is highly suitable for a range of biological uses. An innovation includes replacing calcium ions in HAp with physiologically important elements such as magnesium and zinc [2]. This alteration not only improves the characteristics of the material but also corresponds with the increasing focus on sustainable and biomimetic materials.

Magnesium-substituted hydroxyapatite (Mg-HAp) is well-known for its role in cellular and bone metabolism [3]. It has enhanced biocompatibility and osteoconductivity in comparison to pure hydroxyapatite. The research has shown favourable outcomes in expediting bone healing and mitigating inflammation.

Zinc is necessary for the process of tissue repair and regeneration. Zinc-substituted hydroxyapatite (Zn-HAp) exhibits improved antibacterial characteristics, which makes it appropriate for use in implant dentistry and wound healing processes [4]. The addition of magnesium and zinc to hydroxyapatite presents a wide range of possibilities in the fields of orthopaedics, dentistry and tissue engineering and medication delivery [5,6]. Benefits of magnesium and zinc substituted hydroxyapatite improved biocompatibility, ability to kill germs, faster growth of new bone tissue [7].

Recently, there has been a change in attention towards sustainable and environment friendly techniques of synthesis, which make use of readily available natural materials [8]. The rising incidence of orthopaedic, dental and tissue engineering difficulties has led to a boom in the need for biocompatible materials that can interact seamlessly with the human body. The production of hydroxyapatite using conventional chemical precursors often requires energy-intensive methods and results

in the generation of hazardous byproducts [9]. The use of environmental friendly resources, such as agricultural waste, industrial leftovers and natural minerals, provides a sustainable option. This strategy not only decreases the negative effects on the environment but also offers a cost-efficient technique for producing hydroxyapatite.

The quest for sustainable and environmentally benign materials has intensified the exploration of alternative precursors. Banana plants, ubiquitous in many tropical and subtropical regions, offer a compelling resource. Specifically, the banana flower, often discarded as waste, harbours a treasure trove of bioactive compounds. Banana flowers are a veritable repository of organic acids, flavonoids and minerals. These compounds, renowned for their antioxidant and anti-inflammatory properties, have shown potential in various applications [10,11]. Their incorporation into materials synthesis impart unique functional characteristics. Beyond the scientific intrigue, utilizing banana flower extract aligns with sustainability principles. By transforming agricultural wastes into a valuable resource, this approach contributes to waste reduction and circular economy practices. Moreover, the widespread availability of banana plants makes this approach economically viable.

Despite its great biocompatibility, hydroxyapatite (HAp) has low mechanical strength and is readily fragile [12]. As a result, its use is limited when it comes to supporting weight in bone deformities. In order to address this constraint, researchers have directed their efforts towards developing composites based on HAp by integrating synthetic polymers. Poly(lactic-co-glycolic) acid (PLGA) has also gained recognition for its ability to degrade naturally, its strong mechanical qualities and its biocompatibility [13]. By integrating the osteoconductive capabilities of HAp with the mechanical robustness of PLGA, these composites have the potential to develop biomaterials which may effectively tackle the difficulties related to bone tissue regeneration.

This study introduces a novel approach to develop a sustainable and biocompatible nanocomposite by integrating magnesium and zinc substituted hydroxyapatite (MZHAp) synthesized using banana flower extract (BFE) with the biodegradable polymer poly(lactic-co-glycolic) acid (PLGA). This innovative combination aims to develop a promising material for the biomedical applications.

EXPERIMENTAL

Analytical grade magnesium chloride, zinc chloride, poly-lactic-co-glycolic acid (PCL) and ammonium dihydrogen phosphate ($\text{NH}_4\text{H}_2\text{PO}_4$) was procured from Himedia, India. Double-distilled water was used throughout the experimental work.

Preparation of bananas flower extract: Fresh flowers of bananas (10 g) was washed thoroughly with tap water and then extracted with 200 mL of double-distilled water at 100 °C for 1 h while being swirled using a magnetic stirrer. After cooling, the liquid was filtered using Whatman filter paper to remove any remaining contaminants. The extract was eventually kept until later usage at 5 °C.

Synthesis of biocomposite: A precursor solution containing 0.9 M calcium, 0.05 M magnesium and 0.05 M zinc ions was prepared by dissolving the respective salts in double-distilled water. Subsequently, 0.6 M ammonium dihydrogen phosphate was added dropwise under sonication for 4 h, resulting in a (Ca + Mg + Zn)/P molar ratio of 1.67. The pH of the solution was adjusted to 9 using liquid ammonia followed by the addition of the BFE extract dropwise to the prepared MZHAp solution and sonicated for 30 min. Following, 1 mg of PLGA was slowly added to the MZHAp-BFE solution under vigorous sonication for 1 h. The resulting solution was filtered and dried to obtain the MZHAp-BFE-PLGA biocomposite. For comparison, MZHAp was prepared following the same procedure without the addition of BFE and PLGA.

Characterization: The study used various methods to analyze the mechanical performance of biocomposites. FT-IR spectra were measured using a Perkin-Elmer spectrometer, while X-ray diffraction patterns were analyzed using a Rigaku diffractometer. The morphology and elemental composition of biocomposites samples were examined using scanning electron microscopy with energy dispersive X-ray analysis (SEM-EDAX, JEM-1011). Vickers microhardness tests were conducted on the samples, determining their original state and averaging seven measurements taken at different locations.

Antibacterial activity: The biocomposite samples were evaluated for antibacterial activity against *S. aureus* and *E. coli* using disk diffusion testing at different doses on Muller-Hinton agar. Concentrated cultures of the microorganisms were introduced and the plates were air-dried and left undisturbed for 15 min. Disks were made from Whatman filter paper and incubated at 37 °C for one day. The antibacterial activity was assessed by measuring the zone of inhibition (mm) surrounding the disk.

Cell viability assay: The study involves the cultivation of osteoblasts, especially MG63 cells, in standard culture media, DMEM, which was supplemented with penicillin, streptomycin and 10% FBS. The cells were kept in a humidified environment at 37 °C for 2 days before being removed and treated with trypsin EDTA. The vitality of the cells was assessed using a modified MTT test [14]. To test the cell viability of biocomposites, MG63 osteoblast cells were seeded in 96-well plates at 10^5 cells/mL and treated with MTT solution at 37 °C for 4 h. The solution was then withdrawn, DMSO was added and the plate was agitated for 15 min before measuring absorbance at 570 nm using an ELISA microplate reader.

Acridine orange/propidium iodide (AO/PI) assay: The cell viability was evaluated qualitatively by the AO/PI staining technique. Acridine orange (1 µg/mL) efficiently penetrates cell membranes, staining living cells green, but propidium iodide (1 µg/mL) is impermeable to membranes and only infiltrates cells with damaged membranes, resulting in red staining of dead cells. After biocomposite treatment for 24 h, the cells were treated with a combination of AO and PI. The fluorescence microscopy with a 20× objective and suitable filters was promptly used to observe and take photographs of the stained cells.

Alkaline phosphatase (ALP) assay: A normal growing medium was used to assist the osteoblasts grown in a 96-well

plate. When the cell culture got to 80% confluence, the growing medium was switched out for osteogenic induction media for 1 or 7 days. After being washed twice with PBS, the cells were treated with radioimmunoprecipitation assay (RIPA) buffer. After centrifuging the lysates at 12000 g for 5 min at 4 °C, the liquid that was left over was put on a 96-well plate. The alkaline phosphatase test kit was utilized to assess the activity of ALP for the investigation. The substrate solution (40 μ L) were added to each sample and the plate was then kept at 37 °C for 30 min. The ALP activity was determined by measuring absorbance at 405 nm using a microplate reader.

Osteogenesis assay: The MG63 cells were inoculated in six-well plates and maintained under normal conditions. The cells were either left untreated or subjected to biocomposite treatment for durations of 7 and 14 days. The culture media was renewed every 72 h throughout the trial duration. At the specified time intervals (7 and 14 days), cells were fixed in 70% ethanol at 4 °C for 1 h, then rinsed with distilled water. Cells were then stained with 40 mM alizarin red S at pH 4.2 for 10 min at ambient temperature.

Statistical analysis: Data were expressed as mean \pm standard deviation. Statistical significance was assessed using the Kruskal-Wallis's test, succeeded by Dunn's multiple comparison post-hoc analysis. The threshold for statistical significance was established at $p < 0.05$.

RESULTS AND DISCUSSION

Functional groups analysis: The functional groups of the synthesized materials have been identified by using FTIR spectroscopy. Consistent with the normal spectral profile of HAp [15], the FTIR spectrum of pure MZHAp (Fig. 1a) displayed characteristic bands at 1616, 1425, 1214, 1096 and 954 cm^{-1} , due to the phosphate group (PO_4^{2-}) and bands at 3433 cm^{-1} and 734 cm^{-1} attributed to the hydroxyl group (OH). The characteristic peaks of MZHAp-BFE (Fig. 1b) showed MZHAp as well as extra bands ascribed to BFE. Whereas the peak at 1019 cm^{-1} showed the existence of alkenes inside the BFE extract, the peaks at 2872, 2360 and 1639 cm^{-1} were ascribed to the phenolic compounds [16]. The characteristic peaks connected with MZHAp, BFE and PLGA were identified by the FTIR spectra of the MZHAp-BFE-PLGA composite (Fig. 1c). Attributed to the stretching vibrations of PLGA, the emergence of peaks at 2869, 1639 and 1440 cm^{-1} confirmed its inclusion [17]. A strong interaction between PLGA and the MZHAp-BFE matrix is suggested by the occurrence of these peaks in the composite spectrum. The FTIR analysis confirms the presence of the relevant functional groups and confirms the successful synthesis of the MZHAp-BFE-PLGA composite, with characteristic peaks for MZHAp, BFE and PLGA observed in the composite spectrum suggesting effective integration of the components.

Crystalline phase analysis: The XRD technique was used to analyze the crystalline phases in the synthetic materials. The XRD pattern of pure MZHAp (Fig. 2a) displayed distinct peaks at 2θ values of 25°, 31°, 32°, 42°, 45°, 50°, 55°, 59° and 62°. These values closely matched those specified in the standard JCPDS card No. 09-0432, providing strong evidence for the

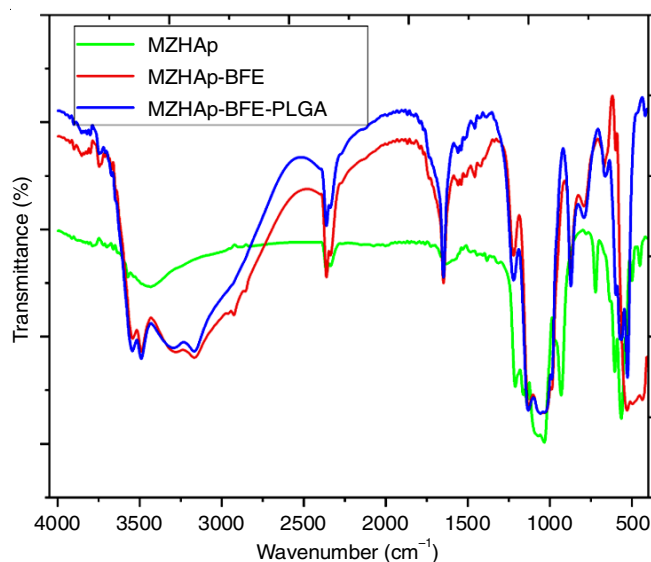


Fig. 1. FTIR spectrum of synthesized biocomposites

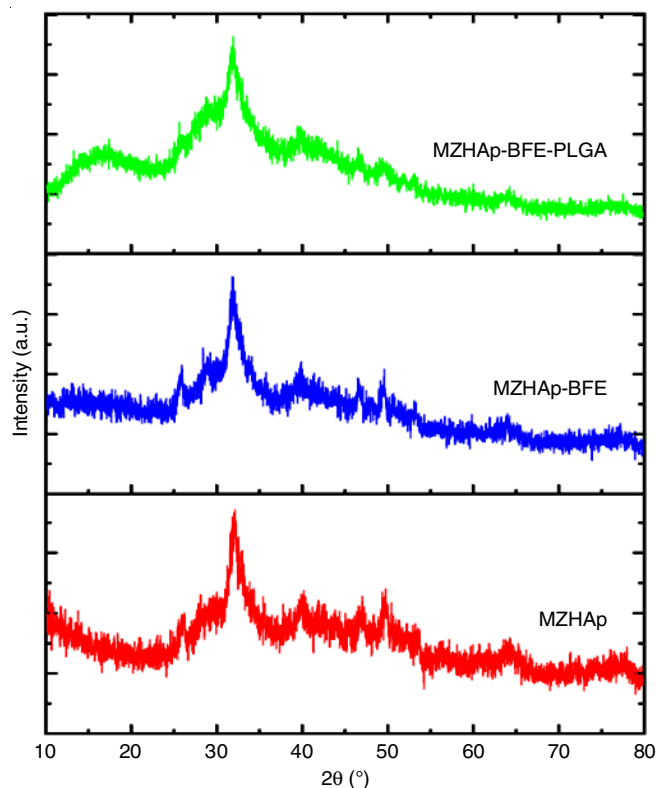


Fig. 2. XRD pattern of synthesized biocomposites

presence of crystalline hydroxyapatite (HAp) [18]. The XRD pattern of MZHAp-BFE exhibited comparable peak locations to pure MZHAp, but with markedly amplified peak intensities, suggesting a significant augmentation in crystallinity. This results indicates that the inclusion of BFE facilitated the formation and enlargement of MZHAp crystals during the synthesis procedure. Significantly, the addition of PLGA did not result in the formation of any additional crystalline structures, indicating that PLGA maintained its amorphous state inside the composite material. The XRD examination verifies the effective formation of crystalline MZHAp and its subsequent alteration by inclu-

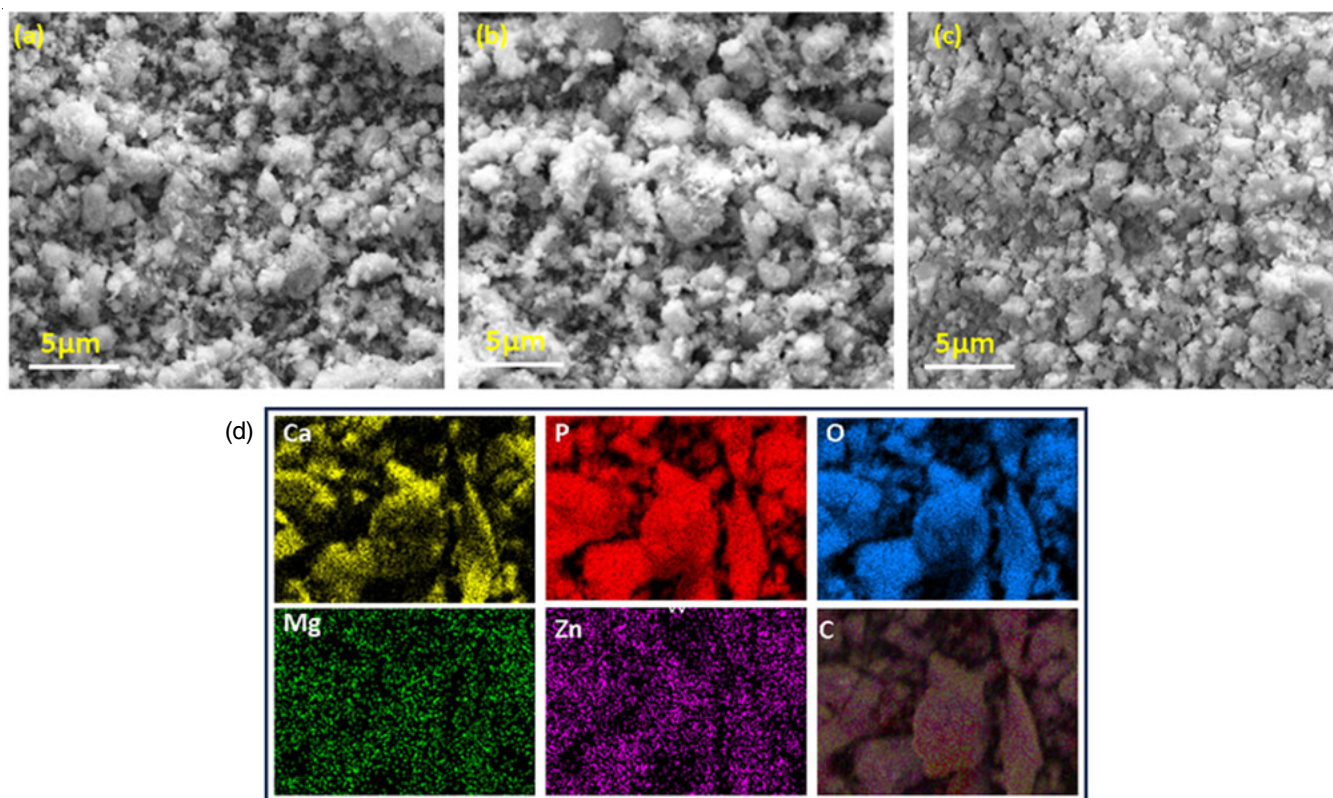


Fig. 3. Morphological images (a) MZHAp, (b) MZHAp-BFE, (c) MZHAp-BFE-PLGA biocomposites and elemental mapping of MZHAp-BFE-PLGA biocomposite

ding BFE and PLGA. The increased crystallinity of MZHAp-BFE is due to the catalytic function of BFE during the process of crystal formation. The absence of a distinct shape or structure of PLGA in the composite is expected to improve the compatibility with biocompatibility of material and its flexibility. The degree of purity and the quality of the crystal structure of the synthesized materials play a critical role in determining their mechanical characteristics, bioactivity and degradation behaviours.

Surface morphology and composition analysis: The surface morphology of synthesized materials using SEM-EDAX showed the distinct morphological characteristics for different samples (Fig. 3). Pure MZHAp had an irregular shaped and highly agglomerated particle structure. The addition of BFE resulted in a well-defined spherical particle with a uniform size distribution, suggesting that the bioactive compounds influenced the nucleation and growth processes of MZHAp particles. The MZHAp-BFE-PLGA composite showed a clustered morphology with uniformly arranged homogeneous particles, indicating successful integration of PLGA into the MZHAp-BFE matrix. Elemental mapping analysis confirmed the presence of Ca, P, Zn, Mg, O and C in the composite. The incorporation of Zn and Mg into the HAp structure confirmed the formation of desired MZHAp composite. The study reveals that the morphological changes and elemental composition of MZHAp-BFE improve its biocompatibility and osteoconductivity.

Microhardness test: The mechanical characteristics of the synthesized materials were assessed by evaluating the Vickers microhardness (Hv) in this work. Fig. 4 suggest that the addition of BFE to MZHAp resulted in a marginal increment in micro-

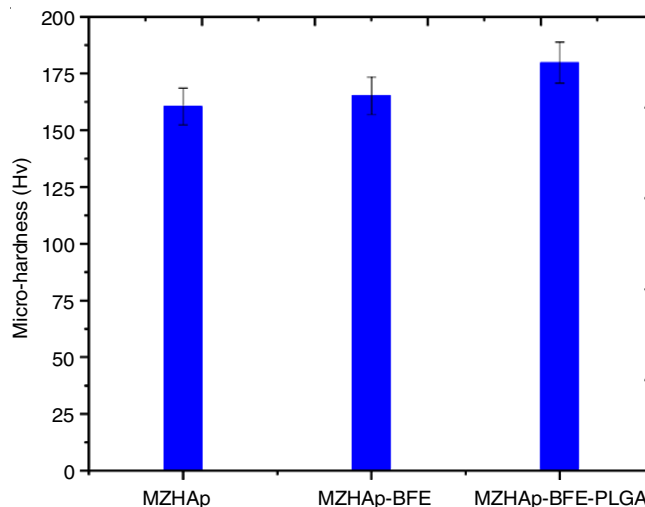


Fig. 4. Mechanical strength of synthesized samples (n = 3)

hardness, increasing from 160.5 Hv for MZHAp to 165.2 Hv for MZHAp-BFE. The MZHAp-BFE-PLGA composite had the greatest microhardness of 179.8 Hv, indicating that the addition of PLGA greatly enhanced the mechanical characteristics of material. The enhanced hardness of the MZHAp-BFE-PLGA composite may be ascribed to the inclusion of PLGA, a polymer renowned for its robust mechanical properties. The even dispersion of PLGA throughout the composite matrix is likely responsible for the observed increase in microhardness. The results align with other research that has shown the beneficial impact of polymer reinforcement on the mechanical chara-

cteristics of the bioceramic composites [19,20]. The enhanced mechanical characteristics of the MZHAp-BFE-PLGA composite make it highly suitable for applications in bone tissue engineering. These qualities have the potential to increase the ability of the implanted material to sustain loads and provide better integration with the surrounding bone tissue.

Antibacterials activity: Fig. 5 illustrates the effectiveness of the prepared materials in inhibiting the growth of both Gram-positive (*S. aureus*) and Gram-negative (*E. coli*) bacteria. The MZHAp-BFE-PLGA composite demonstrated significant higher antibacterial activity against Gram-negative bacteria in comparison to Gram-positive bacteria. The increased antibacterial activity may be ascribed to many sources. The incorporation of Mg and Zn ions into the hydroxyapatite (HAp) structure has been shown to provide antibacterial characteristics by disrupting

bacterial cell membranes [21]. Furthermore, earlier study has shown that the bioactive components *viz.* flavonoids and alkaloids present in the BFE, has an ability to eradicate microorganisms [22]. The synergistic effects of these elements within the composite are anticipated to enhance its overall antibacterial efficacy.

The MZHAp-BFE-PLGA composite has shown potent antibacterial action against Gram-negative bacteria, a type of bacteria that are more vulnerable to antibacterial drugs due to their intricate cell wall structure. This is particularly important due to the prevalence of Gram-negative infections in bone wounds and surgical environments. The potential of composite as an antibacterial coating or implant material for orthopaedics could reduce the likelihood of infections after surgery and improve patient outcomes.

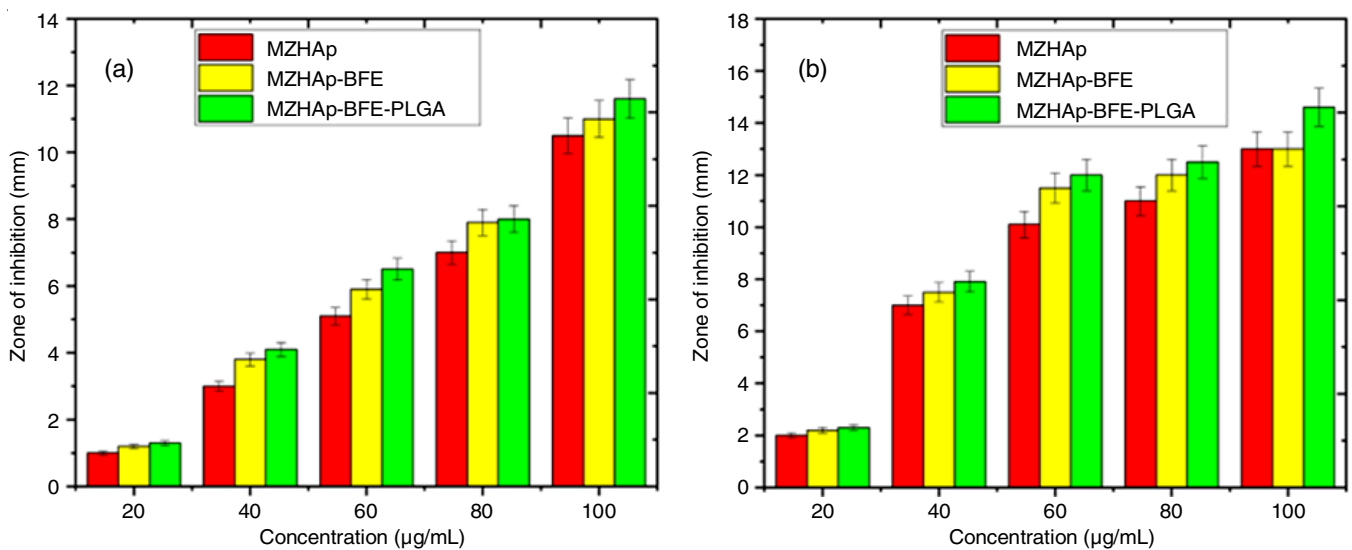


Fig. 5. Bar diagram illustrating biocomposites antibacterial effects against *E. coli* and *S. aureus*

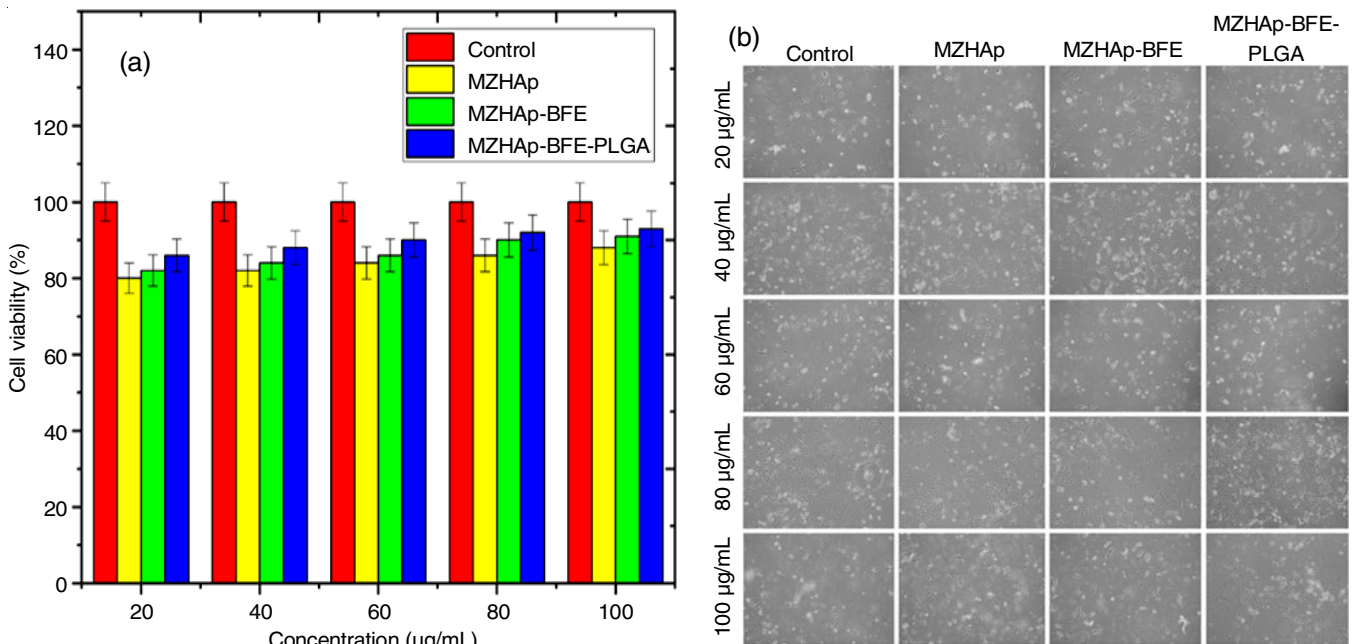


Fig. 6. (a) The MTT assay of MZHAp, MZHAp-BFE and MZHAp-BFE-PLGA biocomposites against MG63 cells over a 24 h period. (b) Micrographs images of cell cytotoxicity using biocomposites. Scale bar: 100 µM

Cell viability assessment: The MTT assay was used to assess the viability of the synthesized biocomposites on MG63 osteoblast cells. The doses tested ranged from 20 to 100 $\mu\text{g}/\text{mL}$. The findings indicate that cell viability increases in a dose-dependent manner (Fig. 6), indicating the exceptional biocompatibility of the prepared material. The MZHAp-BFE-PLGA biocomposite demonstrated enhanced osteocompatibility in comparison to MZHAp. The increased bioactivity may be due to the combined effects of the bioactive constituents found in BFE, such as alkaloids, flavonoids and terpenoids, which have been previously shown to have osteogenic activities [23]. Moreover, the use of PLGA, a well-recognized biocompatible poly-

mer, enhanced the overall biocompatibility of the composite [24]. The composite consisting of bioactive natural extract, biodegradable polymer and mineral phase, seems to provide an ideal environment for the growth and activity of osteoblasts. The *in vitro* cell survival data clearly demonstrate that the MZHAp-BFE-PLGA composite holds significant potential as a viable choice for applications in bone tissue engineering.

Osteoblast cell live/dead assay: The AO/PI staining demonstrated a dose-dependent increase in MG63 osteoblast viability (green fluorescence) with escalating concentrations of MZHAp-BFE-PLGA (20-100 $\mu\text{g}/\text{mL}$) (Fig. 7). The combination exhibited significantly higher cell viability compared to

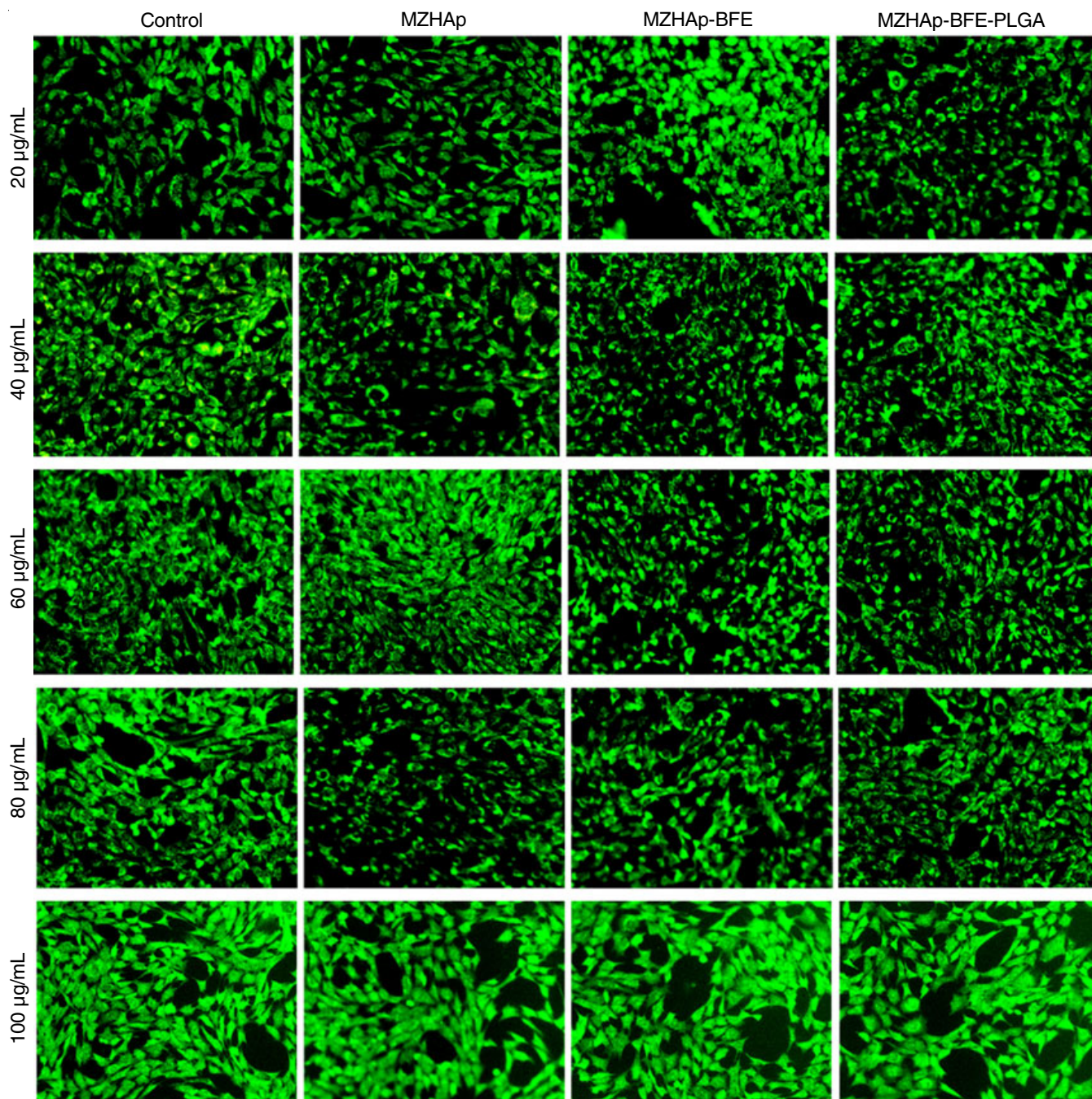


Fig. 7. Fluorescent micrographs depicting AO/PI-stained osteoblasts at 24 h post-treatment (scale bar, 100 μm). Live cells are indicated by green fluorescence, while dead cells are represented by red fluorescence

MZHAp alone, suggesting excellent biocompatibility. This enhancement is likely attributed to the synergistic effects of bioactive compounds within BFE [25]. Moreover, the incorporation of biocompatible PLGA further improved the biocompatibility of composite [26]. The *in vitro* cell survival data strongly indicate the potential of the MZHAp-BFE-PLGA composite for bone tissue engineering applications.

Alkaline phosphatase activity assay: Considered a well-known early indicator of osteoblast development, alkaline phosphatase (ALP) reflects the start of the mineralization process [27]. Days 1 and 7 ALP activity was measured to determine the osteogenic potential of the synthesized materials. All materials were initially biocompatible and did not cause cytotoxicity (Fig. 8), hence ALP activity was not significantly different among the groups on day 1. On day 7, however, ALP activity clearly increased for all groups as compared to day 1, sugges-

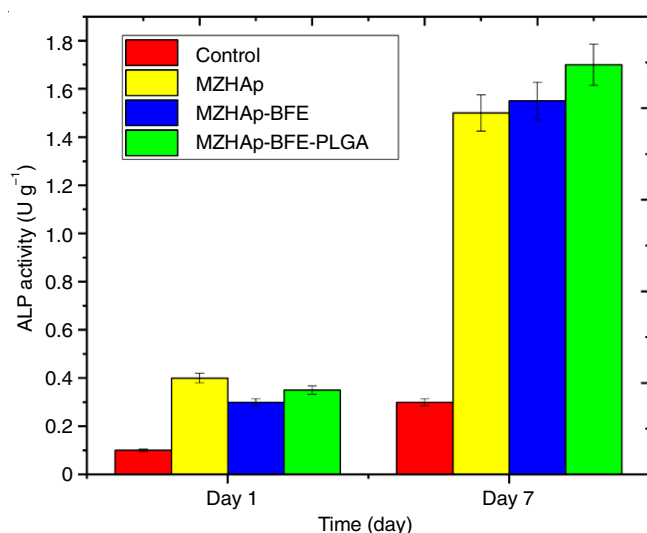


Fig. 8. ALP activity was measured for one and seven days in osteoblasts grown with the inducing media of MZHAp, MZHAp-BFE and MZHAp-BFE-PLGA biocomposites, respectively. The control group consisted of osteoblasts cultured with the inducing medium without any biocomposite

ting the start of osteogenic differentiation. Especially, the composite including MZHAp showed more ALP activity than the control groups, therefore proving the beneficial effect of MZHAp on osteoblast differentiation. Moreover, the inclusion of PLGA to the MZHAp-LA composite produced a greater increase in ALP activity, suggesting that PLGA cooperatively stimulates osteogenesis. These results highly imply that the MZHAp-LA-PLGA composite has outstanding osteogenic characteristics.

Alizarin red S (ARS) mineralization assay: The alizarin red S (ARS) staining test, a recognized marker of early osteoblast development, was used to assess mineralization [28]. Initial *in vitro* evaluations revealed biocompatibility and the lack of cytotoxicity for all materials on day 7, resulting in the minimal variations in ARS activity (Fig. 9). However, a significant increase in the ARS activity was observed across all the groups by day 14, signifying the commencement of osteogenic differentiation. The composite containing MZHAp demonstrated increased ARS activity relative to control groups, highlighting the beneficial effect of MZHAp on osteoblast development. Furthermore, the incorporation of PLGA into the MZHAp-BFE composite enhanced ARS activity, indicating a synergistic interaction between MZHAp and PLGA in promoting osteogenesis. The data combined provide compelling evidence for the enhanced osteogenic capacity of the MZHAp-BFE-PLGA composite.

Conclusion

The present work effectively prepared a new MZHAp-BFE-PLGA biocomposite for application in bone tissue engineering. FTIR analysis verified the existence of the requisite functional groups in the produced materials. XRD examination demonstrated the crystalline characteristics of MZHAp and the amorphous properties of PLGA in the composite. SEM-EDAX analysis demonstrated the effective incorporation of BFE and PLGA into the MZHAp matrix. The biocomposite demonstrated improved the mechanical characteristics, remarkable antibacterial efficacy against Gram-negative bacteria and superior biocompatibility. *In vitro* studies demonstrated enhanced survival of osteoblast cells, increased ALP activity and improved

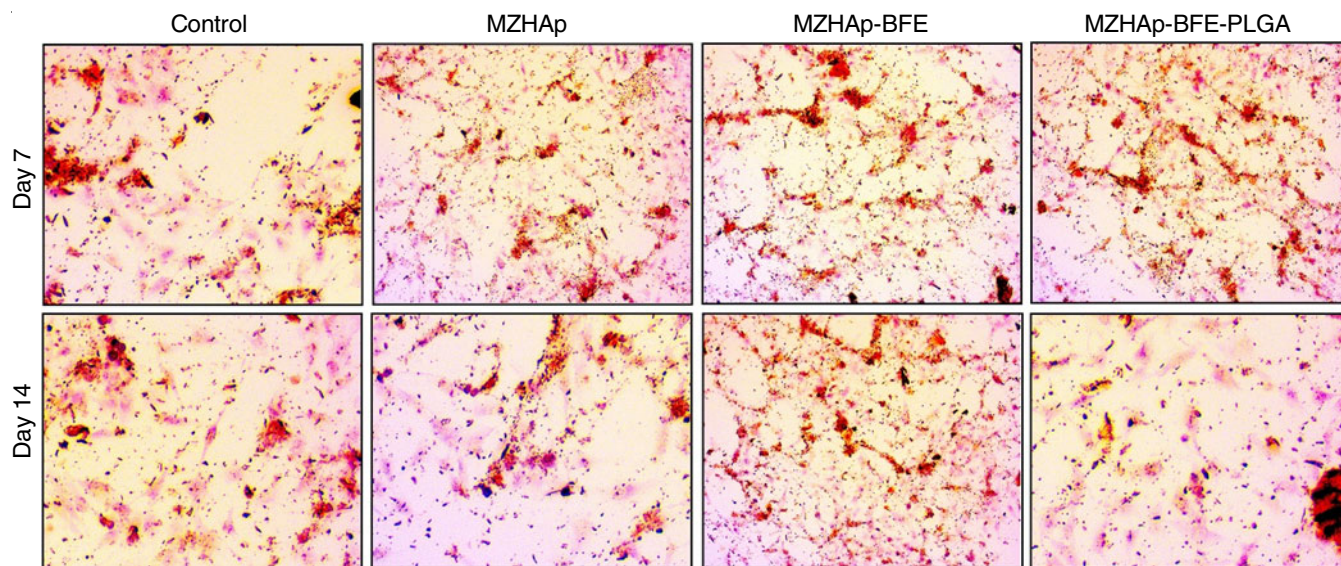


Fig. 9. MG63 cell stained with alizarin red following a 7 to 14-day incubation with the prepared samples

mineralization, indicating the potential capabilities of this bio-composite for regenerating bone tissue.

CONFLICT OF INTEREST

The authors declare that there is no conflict of interests regarding the publication of this article.

REFERENCES

- S. Elbasaney, *J. Inorg. Organomet. Polym. Mater.*, **30**, 899 (2020); <https://doi.org/10.1007/s10904-019-01247-4>
- S.J. Kalita and H.A. Bhatt, *Mater. Sci. Eng. C*, **27**, 837 (2007); <https://doi.org/10.1016/j.msec.2006.09.036>
- A. Mahanty and D. Shikha, *Int. J. Mater. Res.*, **112**, 922 (2021); <https://doi.org/10.1515/ijmr-2020-8181>
- C.O. de Lima, A.L.M. de Oliveira, L. Chantelle, E.C.S. Filho, M. Jaber and M.G. Fonseca, *Colloids Surf. B: Biointerfaces*, **198**, 111471 (2021); <https://doi.org/10.1016/j.colsurfb.2020.111471>
- M. Sartori, G. Giavaresi, M. Tschon, L. Martini, L. Dolcini, M. Fiorini, D. Pressato and M. Fini, *J. Mater. Sci.: Mater. Med.*, **25**, 1495 (2014); <https://doi.org/10.1007/s10856-014-5177-5>
- E. Jallot, J.M. Nedelec, A.S. Grimault, E. Chassot, A. Grandjean-Laquerriere, P. Laquerriere and D. Laurent-Maquin, *Colloids Surf. B: Biointerfaces*, **42**, 205 (2005); <https://doi.org/10.1016/j.colsurfb.2005.03.001>
- X. Wen, J. Wang and X. Zhang, *J. Mater. Chem. B*, **11**, 11405 (2023); <https://doi.org/10.1039/D3TB01874A>
- M.S. Samuel, M. Ravikumar, A. John J, E. Selvarajan, H. Patel, P.S. Chander, J. Soundarya, S. Vuppala, R. Balaji and N. Chandrasekar, *Catalysts*, **12**, 459 (2022); <https://doi.org/10.3390/catal12050459>
- S. Mondal, S. Park, J. Choi, T.T.H. Vu, V.H.M. Doan, T.T. Vo, B. Lee and J. Oh, *Adv. Colloid Interface Sci.*, **321**, 103013 (2023); <https://doi.org/10.1016/j.cis.2023.103013>
- V. Lokesh, P. Divya, B. Puthusseri, G. Manjunatha and B. Neelwarne, *LWT-Food Sci. Technol.*, **55**, 59 (2014); <https://doi.org/10.1016/j.lwt.2013.09.005>
- C.V. Borges, M. Maraschin, D.S. Coelho, M. Leonel, H.A.G. Gomez, M.A.F. Belin, M.S. Diamante, E.P. Amorim, T. Gianeti, G.R. Castro and G.P.P. Lima, *Food Res. Int.*, **132**, 109061 (2020); <https://doi.org/10.1016/j.foodres.2020.109061>
- M.S. Islam, A.Z. Rahman, M.H. Sharif, A. Khan, M. Abdulla-Al-Mamun and M. Todo, *J. Asian Ceramic Soc.*, **7**, 183 (2019); <https://doi.org/10.1080/21870764.2019.1600226>
- E.M. Elmowafy, M. Tiboni and M.E. Soliman, *J. Pharm. Investig.*, **49**, 347 (2019); <https://doi.org/10.1007/s40005-019-00439-x>
- X. Gai, C. Liu, G. Wang, Y. Qin, C. Fan, J. Liu and Y. Shi, *Regener. Biomater.*, **7**, 321 (2020); <https://doi.org/10.1093/rb/rbaa017>
- A.A. Shaltout, M.A. Allam and M.A. Moharram, *Spectrochim. Acta A Mol. Biomol. Spectrosc.*, **83**, 56 (2011); <https://doi.org/10.1016/j.saa.2011.07.036>
- K. Sittthiya, L. Devkota, M.B. Sadiq and A.K. Anal, *J. Food Sci. Technol.*, **55**, 658 (2018); <https://doi.org/10.1007/s13197-017-2975-z>
- J.B. Lee, S.E. Kim, D.N. Heo, I.K. Kwon and B.J. Choi, *Macromol. Res.*, **18**, 1195 (2010); <https://doi.org/10.1007/s13233-010-1206-5>
- R. Murugan and S. Ramakrishna, *Cryst. Growth Des.*, **5**, 111 (2005); <https://doi.org/10.1021/cg034227s>
- M. Hassan, A. Khaleel, S.M. Karam, A.H. Al-Marzouqi, I. Ur Rehman and S. Mohsin, *Polymers*, **15**, 1370 (2023); <https://doi.org/10.3390/polym15061370>
- A.M. Maadani and E. Salahinejad, *J. Control. Release*, **351**, 1 (2022); <https://doi.org/10.1016/j.jconrel.2022.09.022>
- A. Rajendran, S. Balakrishnan, R. Kulandaivelu and S.N.T. Nellaiappan, *J. Sol-Gel Sci. Technol.*, **86**, 441 (2018); <https://doi.org/10.1007/s10971-018-4634-x>
- R. Ramu, P.S. Shirahatti, F. Zameer, D.B. Lakkapa and M. Nagendra, *Int. J. Pharm. Pharm. Sci.*, **7**, 136 (2015).
- R. Rai, S. Kumar, K.B. Singh, S. khanka, Y. Singh, K.R. Arya, S. Kanojjiya, R. Maurya and D. Singh, *Phytomedicine*, **93**, 153750 (2021); <https://doi.org/10.1016/j.phymed.2021.153750>
- R. Pignatello, E. Cenni, D. Micieli, C. Fotia, M. Salerno, D. Granchi, S. Avnet, M.G. Sarpietro, F. Castelli and N. Baldini, *Nanomedicine*, **4**, 161 (2009); <https://doi.org/10.2217/17435889.4.2.161>
- Y. Tang, Z. Wei, X. He, D. Ling, M. Qin, P. Yi, G. Liu, L. Li, C. Li and J. Sun, *Int. J. Biol. Macromol.*, **264**, 130459 (2024); <https://doi.org/10.1016/j.ijbiomac.2024.130459>
- W. Ji, F. Yang, H. Seyednejad, Z. Chen, W.E. Hennink, J.M. Anderson, J.J. van den Beucken and J.A. Jansen, *Biomaterials*, **33**, 6604 (2012); <https://doi.org/10.1016/j.biomaterials.2012.06.018>
- C. Del Giudice, G. Spagnuolo, C. Menale, Y.F. Chou, J.M. Núñez Martí, C. Rengo, S. Rengo and S. Sauro, *Dent. Mater.*, **40**, 2043 (2024); <https://doi.org/10.1016/j.dental.2024.09.019>
- S.H. Zainal Ariffin, R. Megat Abdul Wahab, M. Abdul Razak, M.D. Yazid, M.A. Shahidan, A. Miskon and I.Z. Zainol Abidin, *PeerJ*, **12**, 17790 (2024); <https://doi.org/10.7717/peerj.17790>